NAM

Advanced modelling of URM buildings in support of fragility/consequence functions derivation

Nonlinear dynamic analysis of index buildings for v5 fragility and consequence models

Rui Pinho, Daniele Malomo, Emanuele Brunesi

Date October 2017

Editors Jan van Elk & Dirk Doornhof

General Introduction

The experimental and study program into the seismic response of buildings covers both masonry buildings (Ref. 1 to 8) and concrete buildings (Ref. 9 to 12). These studies result in fragility models for the different building typologies which are used in the hazard and risk assessment.

Results from nonlinear dynamic analysis of multi-degree-of-freedom models of index buildings from the Groningen region were required to develop the fragility and consequences models (Ref. 13) used in NAM's v5 hazard and risk assessment (Ref. 14).

In this report, therefore, the analyses carried out by Mosayk in support of the this v5 fragility/consequence model development are described and discussed. These included both non-URM index buildings (reinforced concrete, steel and timber) analysed with SeismoStruct, as well as URM models analysed with ELS, for a total of 6 case-studies (which, together with another 4 case-studies that had been previously modelled by Mosayk and that did not require updated analysis, complement the additional 9 case-studies modelled by Arup for the same purpose).

References

1. Eucentre Shake-table Test of Terraced House Modelling Predictions and Analysis Cross Validation, staff from ARUP, Eucentre (Pavia) and TU Delft, November 2015 [this document also includes; (1) Instruments full-scale test-house Eucentre Laboratory, (2) Protocol for Shaking Table Test on Full Scale Building (Eucentre) V_1, and (3) Selection of Acceleration Time-Series for Shake Table Testing of Groningen Masonry Building at the EUCENTRE, Pavia, all three by staff from Eucentre (Pavia)],
2. Collapse shake-table testing of terraced house (LNEC-BUILD1), Eucentre and LNEC (U. Tomassetti, A. A. Correia, F. Graziotti, A.I. Marques, M. Mandirola, P.X. Candeias), 1st September 2017.
3. LNEC-BUILD1: Modelling predictions and analysis cross-validation, ARUP, TU Delft, Eucentre and Mosayk (several staff members from all four institutions), 8th September 2017.
4. Using the Applied Element Method to model the collapse shake-table testing of a URM cavity wall structure (LNEC-BUILD1), Mosayk (D. Malomo, R. Pinho), 31st October 2017.
5. Using the Applied Element Method to model the collapse shake-table testing of a terraced house roof substructure (LNEC-BUILD2), Mosayk (D. Malomo, R. Pinho), 31st October 2017.
6. Experimental campaign on a clay URM full-scale specimen representative of the Groningen building stock (EUC-BUILD2), Eucentre (F. Graziotti, U. Tomassetti, A. Rossi, B. Marchesi, S. Kallioras, M. Mandirola, A. Fragomeli, E. Mellia, S. Peloso, F. Cuppari, G. Guerrini, A. Penna, G. Magenes, G), 20th July 2016.
7. EUC-BUILD2: Modelling predictions and analysis cross-validation of detached single-storey URM Building, ARUP, TU Delft, Eucentre and Arcadis (several staff members from all four institutions), 30th September 2016
8. Shake-table test up to collapse on a roof substructure of a Dutch terraced house (LNEC-BUILD2), Eucentre and LNEC (A.A. Correia, A.I. Marques, V. Bernardo, L. Grottoli, U. Tomassetti, F. Graziotti), 31st October 2017.
9. Cyclic testing of precast panel connections for RC precast wall-slab-wall structures representative of the Groningen building stock. Eucentre (E. Brunesi, R. Nascimbene), 22nd October 2015.
10. Cyclic testing of RC tunnel building (EUC-BUILD3), Eucentre (E. Brunesi, S. Peloso, R. Pinho, R. Nascimbene), 8th May 2017.
11. Cyclic testing of RC precast building (EUC-BUILD4), Eucentre (E. Brunesi, S. Peloso, R. Pinho, R. Nascimbene), 22nd June 2017.
12. Shake-table testing of RC precast building (EUC-BUILD5), Eucentre (E. Brunesi, S. Peloso, R. Pinho, R. Nascimbene), 31st October 2017.
13. Report on the v5 fragility and consequence models for the Groningen Field, H. Crowley and R. Pinho, 31st October 2017.
14. Assessment of Hazard, Building Damage and Risk for Induced Seismicity Groningen, November 2017, NAM, Jan van Elk and Dirk Doornhof, November 2017.

NAM

Title	**Advanced modelling of URM buildings in support of fragility/consequence functions derivation** **Nonlinear dynamic analysis of index buildings for v5 fragility and consequence models**		**Date**	October 2017
			Initiator	NAM
Autor(s)	**Rui Pinho, Daniele Malomo, Emanuele Brunesi**	**Editors**	Jan van Elk and Dirk Doornhof	
Organisation	EUCentre	**Organisation**	NAM	
Place in the Study and Data Acquisition Plan	Study Theme: Seismic Response Buildings Comment: The experimental and study program into the seismic response of buildings covers both masonry buildings (Ref. 1 to 8) and concrete buildings (Ref. 9 to 12). These studies result in fragility models for the different building typologies which are used in the hazard and risk assessment. Results from nonlinear dynamic analysis of multi-degree-of-freedom models of index buildings from the Groningen region were required to develop the fragility and consequences models (Ref. 13) used in NAM's v5 hazard and risk assessment (Ref. 14). In this report, therefore, the analyses carried out by Mosayk in support of the this v5 fragility/consequence model development are described and discussed. These included both non-URM index buildings (reinforced concrete, steel and timber) analysed with SeismoStruct, as well as URM models analysed with ELS, for a total of 6 case-studies (which, together with another 4 case-studies that had been previously modelled by Mosayk and that did not require updated analysis, complement the additional 9 case-studies modelled by Arup for the same purpose).			
Directliy linked research	(1) Shake Table Tests (2) Risk Assessment			
Used data	Full experimental and Modelling program into seismic response URM & non-URM buildings.			
Associated organisation	NAM			
Assurance	Independent Assurance Panel			

D8

DELIVERABLE

Project Information

Project Title:	**Advanced modelling of URM buildings in support of fragility/consequence functions derivation**
Project Start:	May 2016
Duration:	20 months
Technical Point of Contact:	Rui Pinho
Administrative Point of Contact:	Roberto Nascimbene

Deliverable Information

Deliverable Title:	**Nonlinear dynamic analysis of index buildings for v5 fragility and consequence models**
Data of Issue:	1st November 2017
Authors:	Rui Pinho, Daniele Malomo, Emanuele Brunesi
Reviewer:	Helen Crowley

REVISION: **31st October 2017**

Table of Contents

Executive Summary

Results from nonlinear dynamic analysis of multi-degree-of-freedom models of index buildings from the Groningen region were required by NAM's Fragility Modelling Team in order to develop the fragility and consequences models used in NAM's v5 hazard and risk assessment.

In this report, therefore, the analyses carried out by Mosayk in support of the aforementioned v5 fragility/consequence model development endeavour are described and discussed. These included both non-URM index buildings (reinforced concrete, steel and timber) analysed with SeismoStruct, as well as URM models analysed with ELS, for a total of 6 case-studies (which, together with another 4 case-studies that had been previously modelled by Mosayk and that did not require updated analysis, complement the additional 9 case-studies modelled by Arup for the same purpose).

1 Introduction

1.1 Scope

The v5 fragility and consequence models used in NAM's v5 hazard and risk assessment are developed using single degree of freedom (SDOF) models. The hysteretic response of these SDOF models is calibrated using the nonlinear dynamic analysis results of multi-degree-of-freedom (MDOF) models of index buildings from the Groningen region (Crowley and Pinho, 2017).

In this report, the MDOF nonlinear dynamic analyses carried out by Mosayk in support of the aforementioned v5 fragility/consequence model development endeavour are described and discussed. These included both non-URM index buildings (reinforced concrete, steel and timber), as well as URM models, for a total of 6 case-studies (which complement the 9 case-studies modelled by Arup (2017a) for the v5 fragility/consequence model development, and an additional 4 case-studies that had been previously modelled by Mosayk (2015), and which did not require updated analysis).

1.2 Structural analysis tools

Two software packages have been used herein to carry out the MDOF nonlinear dynamic analyses: Extreme Loading for Structures (ASI, 2017) for unreinforced masonry (URM) structures and SeismoStruct (Seismosoft, 2017) for reinforced concrete, timber and steel structures.

Extreme Loading for Structures (ELS) is a commercial structural-analysis software based on the Applied Element Method (Meguro and Tagel-Din, 2000, 2001, 2002). This software has been validated against a number of experimental tests, as described in a series of reports by Mosayk (2016, 2017a, 2017b, 2017c, 2017d).

SeismoStruct is an extensively quality-checked and internationally validated Finite Elements software tool able to accurately predict the large displacement behaviour of space frames under static or dynamic loading (e.g. earthquake strong motion), taking into account both geometric nonlinearities and material inelasticity. Further validation of this software is provided in Mosayk (2014).

1.3 Buildings considered

The main objective when modelling index buildings for the fragility function development is to use the geometry and structural elements materials/connections of real buildings that are representative of a given typology of structures. Table 1.1 presents the name, address and description of the index buildings presented herein according to building classification scheme used in both v3 and v5 of the exposure database (Arup, 2017b).

In some cases it has not yet been possible to model real buildings, and so generic structures with typical characteristics of the typology have been modelled instead; these are identified in Table 1.1 as 'generic models'. The ELS model of the URM full-scale specimen that was tested at LNEC (LNEC-BUILD1) has also been included herein, as it was used to investigate the influence of triaxial loading on the collapse capacity.

The presentation of the analyses of the six buildings shown in Table 1.1 has been subdivided into two chapters; the first four are new index buildings and are presented in full in Chapter 2, whereas the last two case-studies, developed previously, have already been described in Mosayk (2015) and thus only the new results now obtained for these models are presented in Chapter 3.

Table 1.1: Overview of the index buildings analysed and their typologies according to the building taxonomies used in both versions 3 and 5 of the exposure database (Arup, 2017b)

Model	Address	Building Typology – EDB v3	Building Typology – EDB v5
Nieuwstraat	Nieuwstraat 8, Loppersum	RESD-URM-A	UHO-MUR/LWAL/MUR/LWAL/EWN/FW
LNEC-BUILD1	N/A (test specimen)	REST-URM-C	UBH-MUR/LWAL/MUR/LN/EW/FC
Pre-cast RC slab-wall	N/A (generic model)	REST-URM-B	UBH-CR+PC/LWAL/CR+PC/LN/EW/FC
Cast-in-place RC slab-wall	N/A (generic model)	REST-URM-A	UBH-CR+CIP/LWAL/CR+CIP/LN/EW/FC
Timber frame/panel	Kwelder 8, Loppersum	RESD-W-A	UHO-W/LWAL/W/LWAL/EW/FW
Light steel braced frame	Beneluxweg 15, Zuidbroek	AIC-S-A	WB-S/LPB/S/LFBR/EWN/FN

1.4 Ground motions

The metadata of the 11 ground motions that have been applied to all models presented herein is given in Table 1.2. These ground motions have been selected to cover a range of intensities, described in terms of AvgSa (Kohranghi et al., 2017), Arias Intensity, PGA and spectral acceleration at 0.1 seconds. The horizontal component described in Table 1.2 has been applied in the weak direction of each model, where this is identified *a priori* as that which is expected to have the lowest strength (i.e. base shear capacity). The other two components (horizontal and vertical) have also been applied to all models. Each record has been truncated (Arup, 2017a) to reduce the run-time of the analyses.

Table 1.2: Summary of ground motions

Ground motion	AvgSa (g)	Arias Intensity (m/s)	PGA (g)	Sa(0.1s)
N_00356L	0.07	0.07	0.09	0.11
E_00137_EW	0.09	0.26	0.19	0.44
N_00694T	0.14	0.46	0.23	0.38
N_00616T	0.22	0.49	0.24	0.49
N_00147T	0.27	0.51	0.25	0.67
N_00250L	0.34	1.53	0.88	0.87
E_17167_EW	0.40	1.20	0.53	0.72
N_00415L	0.46	1.74	0.70	1.02
N_00569T	0.46	2.25	0.52	0.68
N_00407L	0.57	3.54	0.82	1.26
N_00451T	0.74	3.85	1.25	1.49

2 New Index Building Models and Results

2.1 Nieuwstraat

Nieuwstraat is an unreinforced masonry detached house with timber attic and roof diaphragms built around 1940. A model of this building has been developed with LS-DYNA (as described in Arup, 2017a), and it was found to have a collapse mechanism that had not been observed in other models or tests. Hence, for cross-validation purposes, an ELS model was also developed by Mosayk (Figure 2.1), and the corresponding capacity and debris area results were used by NAM's Fragility Modelling team.

Figure 2.1: Nieuwstraat 8 house from Google Street View (left) and the corresponding ELS model (right) – note that roof tile elements are not shown in the ELS model, so as to allow the visualisation of the roof structure

2.1.1 Modelling assumptions

Table 1.1 summarises the main characteristics and modelling assumptions for this index building and typology.

Table 2.1: Nieuwstraat – Summary of the building model information

Typology (v3 | v5)	RESD-URM-A | UHO-MUR/LWAL/MUR/LWAL/EWN/FW
Number of storeys	1 (plus attic)
Height	6.35 m
Directions	Weak = gable wall acts out-of-plane, Strong = gable wall acts in-plane
Walls	Exterior walls: Solid walls (210 mm thickness) Interior walls: Solid walls (100 mm thickness)
Floors	Attic floor: timber diaphragms; floor secondary beams span primary beams and walls parallel to the weak axis. Primary beams span onto internal and external walls parallel to the strong axis.
Roof	Roof tiles modelled as an equivalent plane element. Each roof timber beam modelled as a continuous element (i.e. no nailed connections considered between the beam segments).
Roof to wall connection	Equivalent mortar spring layer
Floor to wall connection	Equivalent mortar spring layer (no blind anchors were modelled)
Floor to roof connection	No connection
Total mass (weight)	100 t
Footprint area	70 m^2
Masonry material properties	Inferred considering the parameters provided in Arup (2017a) for clay pre-1945

2.1.2 Summary of results

Displacement and base shear results for the weak and strong directions are summarised in Table 2.2, with the observed collapse mechanisms described in Table 2.3 being shown in Figure 2.2 to Figure 2.4. The hysteresis plots of all 11 records are shown in Figure 2.5 and Figure 2.6 for the weak and strong directions, respectively.

Table 2.2: Nieuwstraat – Summary of the numerical results

Ground motion	AvgSa [g]	Weak direction		Strong direction	
		Peak ref. node displacement (pre-collapse*) [mm]	Peak base shear (pre-collapse*) [kN]	Peak ref. node displacement (pre-collapse*) [mm]	Peak base shear (pre-collapse*) [kN]
N_00356L	0.07	1	44	0.1	31
E_00137_EW	0.09	3	72	0.5	154
N_00694T	0.14	3	102	0.6	110
N_00616T	0.22	5	108	0.5	72
N_00147T	0.27	5	137	0.7	103
N_00250L	0.34	26	182	2.5	190
E_17167_EW	0.40	43	234	1.5	240
N_00415L	0.46	52	192	10	321
N_00569T	0.46	104	229	5.7	187
N_00407L	0.57	35	206	3.6	209
N_00451T	0.74	164	280	6.0	268

* pre-collapse response values stand for: (i) either peak values observed during the entire analyses when no collapse occurs, or (ii) response values at the instant immediately before collapse occurs

Table 2.3: Nieuwstraat – Summary of the collapse mechanisms

Ground motion	Description of response /collapse mechanism
N_00356L	No damage.
E_00137_EW	Partial unseating of main floor beam, but not such as to induce collapse of the floor.
N_00694T	Partial unseating of main floor beam, but not such as to induce collapse of the floor.
N_00616T	Partial unseating of main floor beam, but not such as to induce collapse of the floor.
N_00147T	Partial unseating of main floor beam, but not such as to induce collapse of the floor.
N_00250L	Out-of-plane response of the end (gable) walls causes the main floor beam to unseat leading to 90% of the floor collapsing
E_17167_EW	Partial unseating of main floor beam, but not such as to induce collapse of the floor.
N_00415L	Out-of-plane response of the end (gable) walls causes the main floor beam to unseat leading to 90% of the floor collapsing. Small part of the wall lintels collapse both inside and outside the building.
N_00569T	Global collapse, initiates at around 5 seconds.
N_00407L	Out-of-plane response of the end (gable) walls causes the main floor beam to unseat leading to 90% of the floor collapsing. Small part of the wall lintels collapse both inside and outside the building.
N_00451T	Global collapse (though the end walls remain standing).

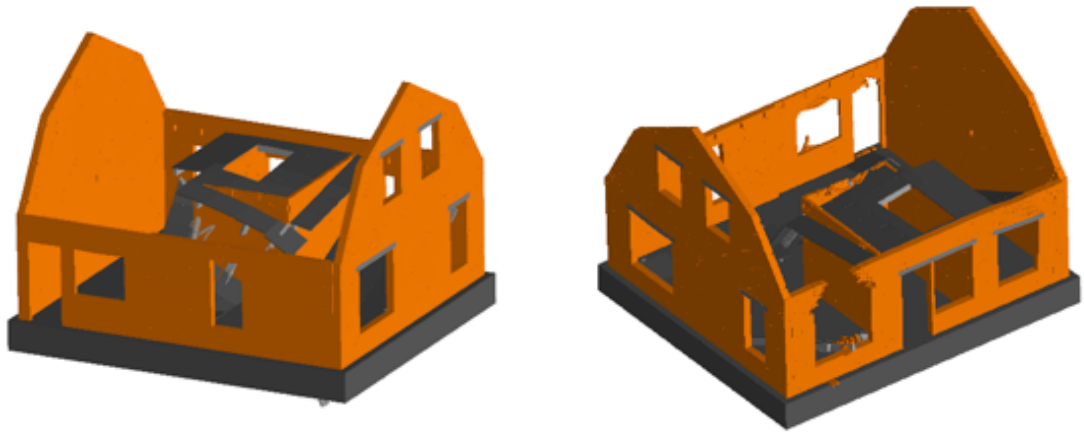

Figure 2.2: Nieuwstraat – Screenshots of collapse mechanisms under record N_00250L (left) and N_00415L (right)

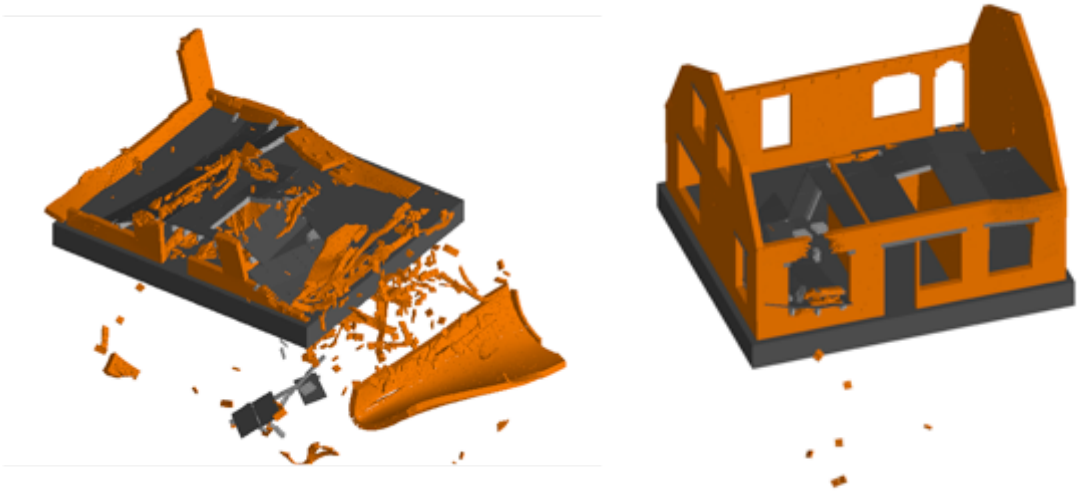

Figure 2.3: Nieuwstraat – Screenshots of collapse mechanisms under record N_00569T(left) and N_00407L (right)

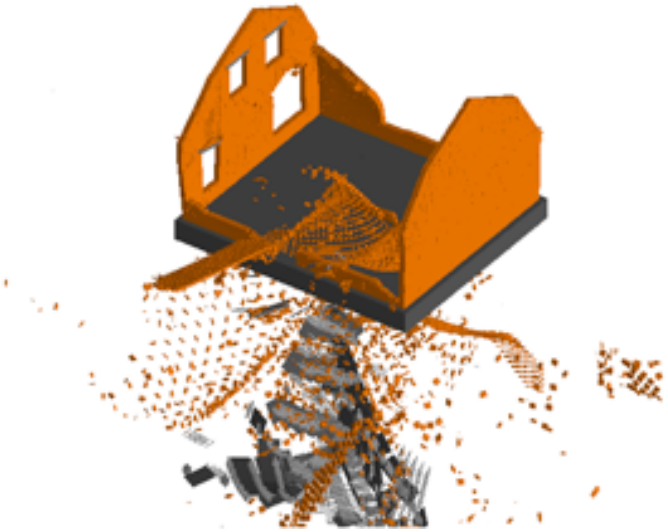

Figure 2.4: Nieuwstraat – Screenshot of collapse mechanism under record N_00451T

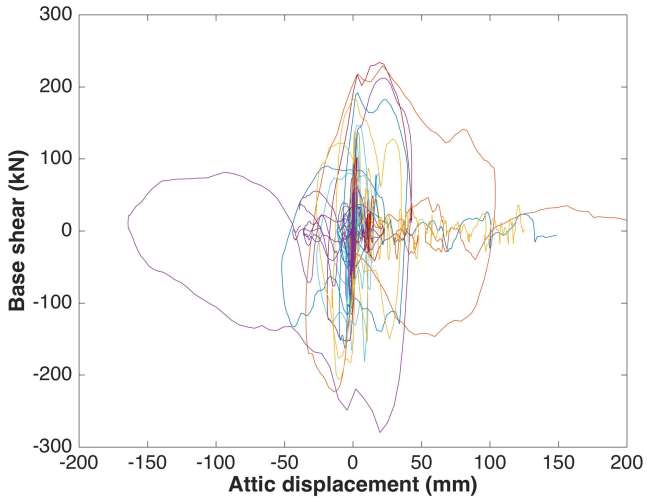

Figure 2.5: Nieuwstraat – Hysteresis plots of the 11 recordings in the weak direction

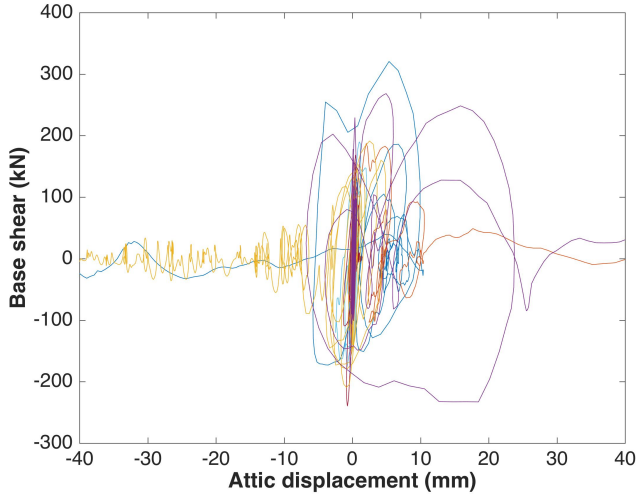

Figure 2.6: Nieuwstraat – Hysteresis plots of the 11 recordings in the strong direction

2.2 LNEC-BUILD1

A full-scale URM cavity wall house specimen (LNEC-BUILD1) was tested in 2017 at the shake-table of the Laboratório Nacional de Engenharia Civil (LNEC - Lisbon, Portugal) under the coordination of the European Centre of Training and Research in Earthquake Engineering (Eucentre - Pavia, Italy) – see report by Tomassetti et al. (2017). It represents the top floor and roof of terraced housing with cavity walls and concrete diaphragms.

Since the shake-table test considered ground shaking in two directions only (in the weak horizontal direction and the vertical direction), it was important for NAM's Fragility Modelling Team to check if the seismic capacity values observed during the test (and in particular the displacement values at different damage/collapse limit states) would change significantly when triaxial loading was applied to the structure. Hence, an ELS model of the test specimen, fully validated against the experimental results (see Mosayk, 2017b), was herein subjected to the 11 records presented in Section 1.4.

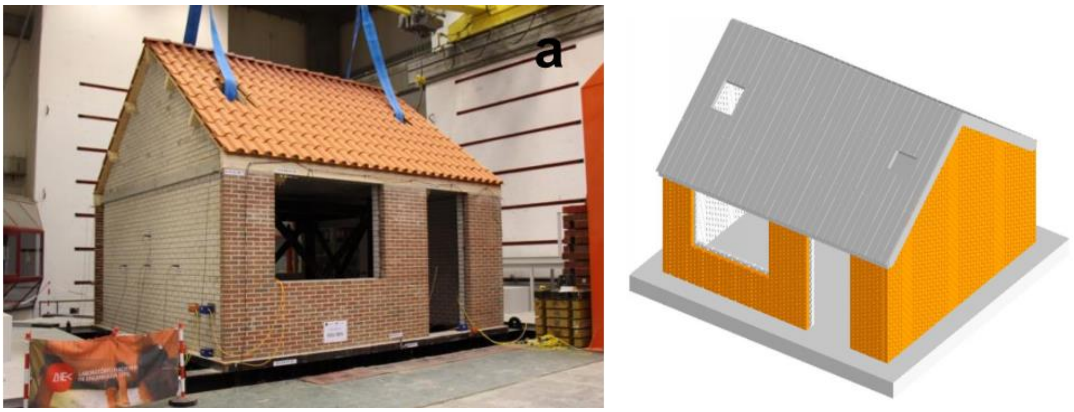

Figure 2.7: LNEC-BUILD1 test specimen (left) and the corresponding ELS model (right)

2.2.1 Modelling assumptions

Table 2.4 summarises the main characteristics and modelling assumptions for this type of building typology.

Table 2.4: LNEC-BUILD1– Summary of the building model information

Typology (v3 | v5)	REST-URM-C | UBH-MUR/LWAL/MUR/LN/EW/FC
Number of storeys	1 (plus attic)
Height	4.93 m
Directions	Weak = gable wall acts out-of-plane, Strong = gable wall acts in-plane
Walls	100 mm calcium-silicate brick plus 100 mm clay bricks with 80 mm air cavity in-between leafs
Floors	Concrete slab
Roof	Nailed connections between timber planks and beams modelled as equivalent spring interfaces characterised by an elastic-perfectly-plastic behaviour
Roof to wall connection	Cracked mortar interface accounting for the damage occurred during transportation phases (active after the static/gravity loading stage)
Floor to wall connection	Cracked mortar interface accounting for the damage occurred during transportation phases (active after the static/gravity loading stage) for the end/party walls, whereas a mortar interface was assigned to front-back walls
Floor to roof connection	Elastic perfectly-plastic interface
Total mass (weight)	31 t
Footprint area	32 m^2
Masonry material properties	Inferred considering the parameters provided in the test report by Tomassetti et al. (2017) and reported also in Arup (2017c).

2.2.2 Summary of results

Displacement and base shear results for the weak and strong directions are summarised in Table 2.2, whilst the hysteresis plots of all 11 records are shown in Figure 2.8 and Figure 2.9. Considering the aforementioned goal of the analyses of this particular structure (i.e. check if the seismic capacity values observed during the testing of the LNEC-BUILD1 specimen would change significantly when triaxial loading was considered), collapse modes and debris area needed not to be scrutinised, this being the reason why they are not included herein.

Table 2.5: LNEC-BUILD1 – Summary of the numerical results

Ground motion	AvgSa [g]	Weak direction		Strong direction	
		Peak ref. node displacement (pre-collapse*) [mm]	Peak base shear (pre-collapse*) [kN]	Peak ref. node displacement (pre-collapse*) [mm]	Peak base shear (pre-collapse*) [kN]
N_00356L	0.07	1	28	0.0	20
E_00137_EW	0.09	15	80	0.4	103
N_00694T	0.14	4	84	0.1	75
N_00616T	0.22	12	116	0.6	54
N_00147T	0.27	22	103	1.9	81
N_00250L	0.34	42	144	3.7	123
E_17167_EW	0.40	60	168	2.2	156
N_00415L	0.46	111	158	4.8	229
N_00569T	0.46	120	146	11	133
N_00407L	0.57	66	148	1.9	146
N_00451T	0.74	135	120	13	176

* pre-collapse response values stand for: (i) either peak values observed during the entire analyses when no collapse occurs, or (ii) response values at the instant immediately before collapse occurs

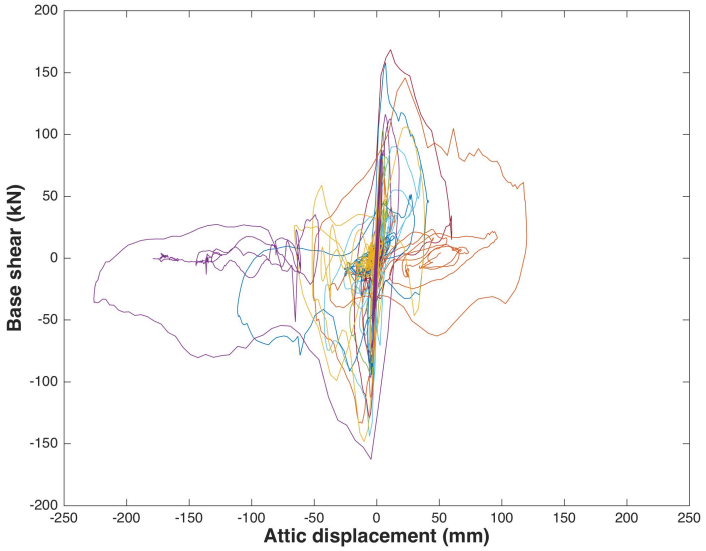

Figure 2.8: LNEC-BUILD1 – Hysteresis plots of the 11 recordings in the weak direction

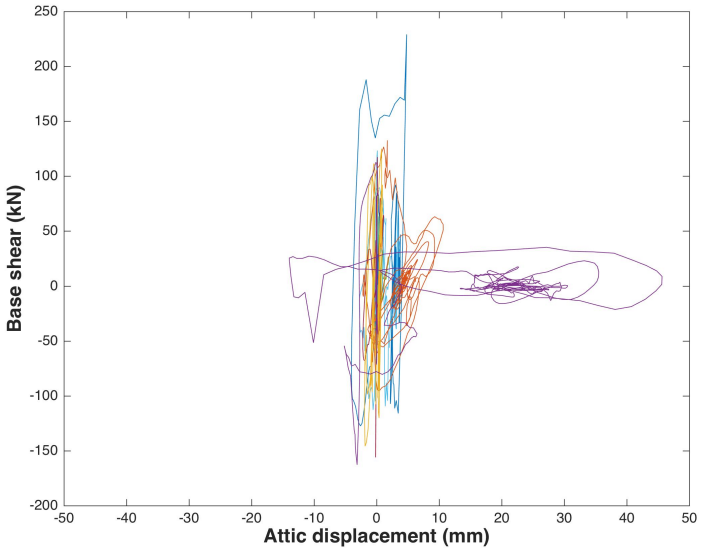

Figure 2.9: LNEC-BUILD1 – Hysteresis plots of the 11 recordings in the strong direction

2.3 Precast (PC) Reinforced Concrete (RC) Wall-Slab Building

Complete details (which would e.g. feature information on both bearing and non-bearing walls) for a precast reinforced concrete wall-slab index building were not available during the development of the current study, and hence the analyses undertaken could only focus on the seismic response of a typical structural configuration of the load-bearing structural elements for this type of buildings.

Such structural configuration was taken from the report by Arup (2017d), which considered typical geometrical and connection properties of a prototype structure for this typology of buildings, leading to the model shown in Figure 2.10. Two full-scale test specimens based on this prototype were tested cyclically and dynamically at Eucentre (see Brunesi et al., 2017a, 2017b), and hence it was possible to use the corresponding experimental results to validate and calibrate the numerical model employed in this study.

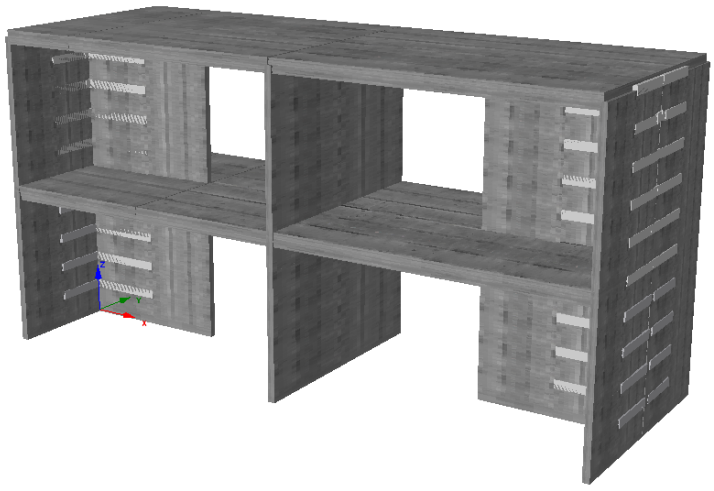

Figure 2.10: SeismoStruct model of the precast RC wall-slab building

2.3.1 Modelling assumptions

Table 2.6 summarises the main characteristics and modelling assumptions for this type of structural typology.

Table 2.6: PC RC Wall-Slab building – Summary of the building model information

Typology (v3 | v5)	REST-URM-B | UBH-CR-PC/LWAL/CR-PC/LN/EW/FC
Number of storeys	2 storeys
Height	5.52 m
Directions	Weak = party walls act out-of-plane, Strong = party walls act in-plane
Walls	120 mm thick stability and transversal walls modelled as a series of displacement-based fibre beam elements with material properties that are calibrated according to material characterisation tests (see Eucentre 2017a and 2017b).
Floors	200 mm thick hollow core slab panels (plus a 50 mm thick concrete screed). Use is made of a series of equivalent elastic beam elements, with stiffness that accounts for the presence of both voids and concrete topping.
Floor to wall connection	Connections between foundation/slabs and transverse walls are modelled by means of inelastic displacement-based fibre beam elements, with material properties that are calibrated in accordance with the material characterisation test results (see Eucentre 2017b). The connections between the first-storey slab and the stability walls are modelled by means of equivalent inelastic links, again calibrated according to the material characterisation test results (see Eucentre 2017b).
Wall to wall connections	Wall to wall connections are modelled by means of inelastic displacement-based fibre beam elements, which are connected to the structural wall elements by means of rigid elements and constraints. The steel material stress-strain relationship is calibrated according to the material characterisation testing of the steel connectors (see Eucentre 2017a).
Total mass (weight)	99 t
Footprint area	44 m^2
Concrete material properties	Material mechanical properties were inferred considering the parameters found in Eucentre (2017b); it is nonetheless noted that material properties of concrete have little influence on the response of this type of structures, whose seismic response is mostly governed by the behaviour of the element connections.

As mentioned previously, results from lab tests on two full-scale test specimens that were based on the prototype structure being analysed herein were available and employed in the validation/calibration of the modelling strategy and assumptions summarised in Table 2.6 above – some comparisons between the experimental and numerical results are shown in Figure 2.11 to Figure 2.13, where it can be observed that the model is able to capture the response of these structural systems in both elastic (Figure 2.11) as well as inelastic (Figure 2.12) ranges, as well as in the post-peak softening/failure stage (Figure 2.13).

From Figure 2.13 one may also appreciate that once the cohesion (mobilised by felt friction resistance or by strength of mortar, whichever the two are present) between stability walls and floor slabs is overcome (in the test case this happened at around 20 mm of displacement) the structure experiences a significant loss of strength and stiffness, which may then rapidly lead to a collapse situation (due to unseating of the floors).

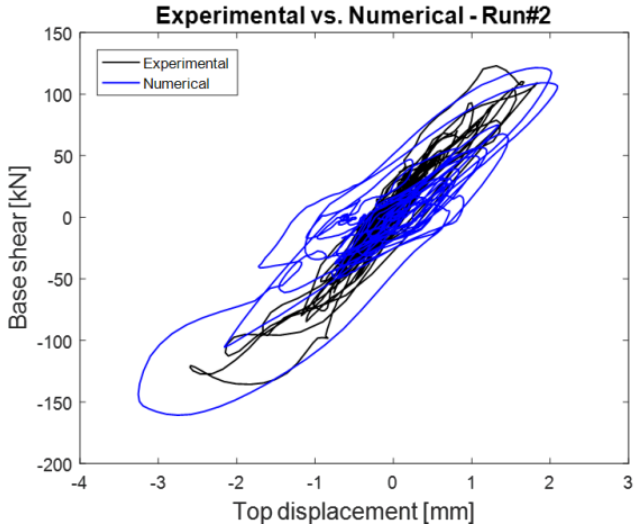

Figure 2.11: Comparison between experimental and numerical results – EUC-BUILD5 specimen, test run #2

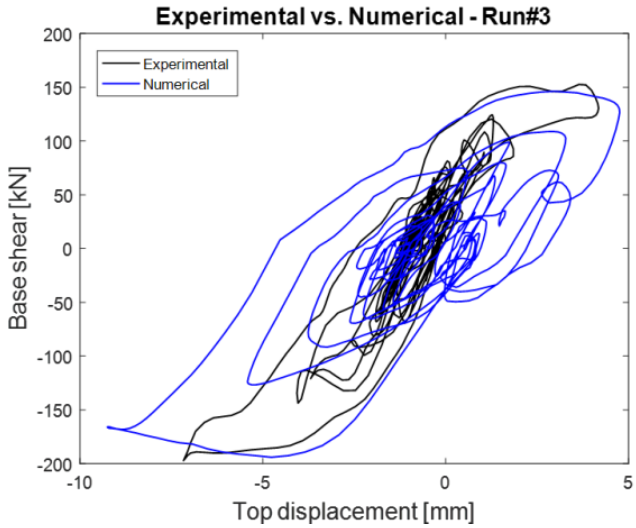

Figure 2.12: Comparison between experimental and numerical results – EUC-BUILD5 specimen, test run #3

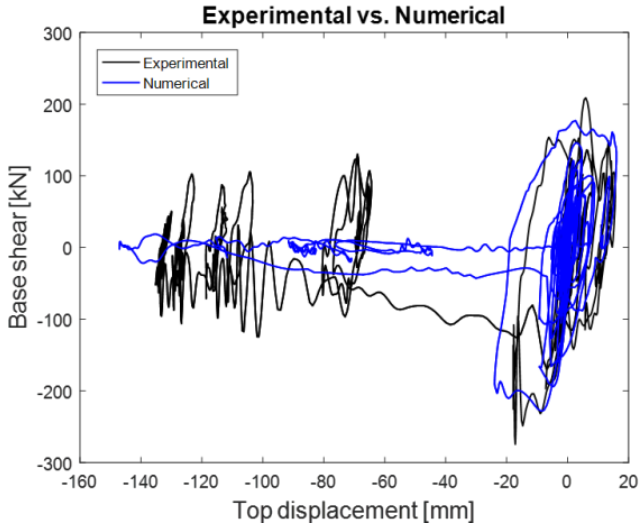

Figure 2.13: Comparison between experimental and numerical results – EUC-BUILD5 specimen, full test sequence

2.3.2 Summary of results

Displacement and base shear results for the weak and strong directions are summarised in Table 2.7, whilst the observed response and collapse mechanisms are described in Table 2.8. The hysteresis plots of all 11 records are shown Figure 2.14 and Figure 2.15 for the weak and strong directions, respectively.

Table 2.7: PC RC Wall-Slab building – Summary of the numerical results

Ground motion	AvgSa [g]	Weak direction		Strong direction	
		Peak ref. node displacement (pre-collapse*) [mm]	Peak base shear (pre-collapse*) [kN]	Peak ref. node displacement (pre-collapse*) [mm]	Peak base shear (pre-collapse*) [kN]
N_00356L	0.07	1	114	0.0	72
E_00137_EW	0.09	3	279	0.3	323
N_00694T	0.14	2	217	0.2	231
N_00616T	0.22	5	318	0.1	150
N_00147T	0.27	5	326	0.2	209
N_00250L	0.34	52	410	59	388
E_17167_EW	0.40	26	497	31	484
N_00415L	0.46	18	414	2	600
N_00569T	0.46	120	412	124	277
N_00407L	0.57	55	477	47	344
N_00451T	0.74	135	635	68	570

* pre-collapse response values stand for: (i) either peak values observed during the entire analyses when no collapse occurs, or (ii) response values at the instant immediately before collapse occurs

Table 2.8: PC RC Wall-Slab building – Summary of the collapse mechanisms

Ground motion	Description of response /collapse mechanism
N_00356L	No damage.
E_00137_EW	No damage.
N_00694T	No damage.
N_00616T	Minor cracking of slab-to-wall and wall-to-wall joints.
N_00147T	Minor cracking of slab-to-wall and wall-to-wall joints.
N_00250L	Significant sliding between slabs and walls, and rupture of wall-to-wall connectors.
E_17167_EW	Moderate sliding between slabs and walls, and yielding of wall-to-wall connectors.
N_00415L	Heavy cracking of slab-to-wall and wall-to-wall joints, and yielding of wall-to-wall connectors.
N_00569T	Collapse due to slab unseating.
N_00407L	Significant sliding between slabs and walls, and rupture of wall-to-wall connectors.
N_00451T	Collapse due to slab unseating.

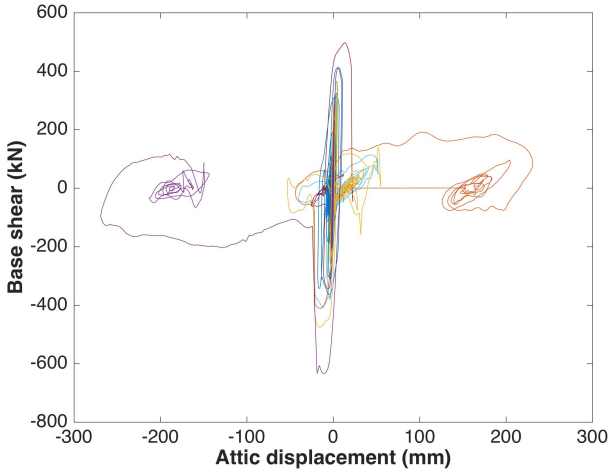

Figure 2.14: PC RC Wall-Slab building – Hysteresis plots of the 11 recordings in the weak direction

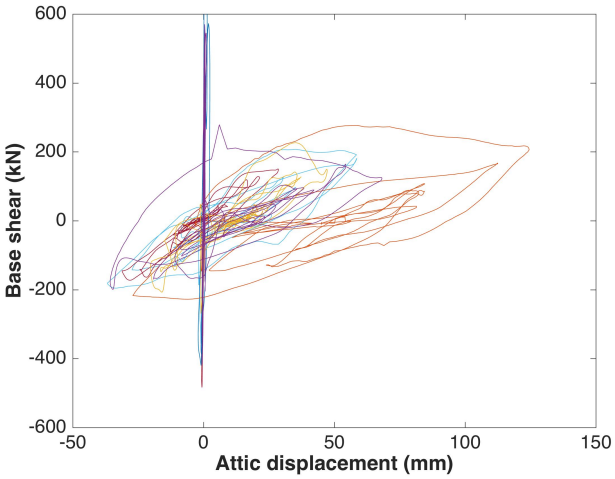

Figure 2.15: PC RC Wall-Slab building – Hysteresis plots of the 11 recordings in the strong direction (note: some apparently spurious response peaks can be observed; these were however not consider by NAM's Fragility Modelling Team)

2.4 Cast-in-place (CIP) RC Wall-Slab Building

Similarly to its precast counterpart, complete details (which would e.g. feature information on both bearing and non-bearing walls) for a cast-in-place reinforced concrete wall-slab index building (often built with the so-called tunnel construction technology) were not available during the development of the current study, and hence the analyses undertaken could only focus on the seismic response of a typical structural configuration of the load-bearing structural elements for this type of buildings.

Such structural configuration was taken from the report by Arup (2017e), which considered typical geometrical and connection properties of a prototype structure for this typology of buildings, leading to the model shown in Figure 2.16. A full-scale test specimen based on this prototype was tested cyclically at Eucentre (see Brunesi et al., 2017c), and hence it was possible to use the corresponding experimental results to validate and calibrate the numerical model employed in this study.

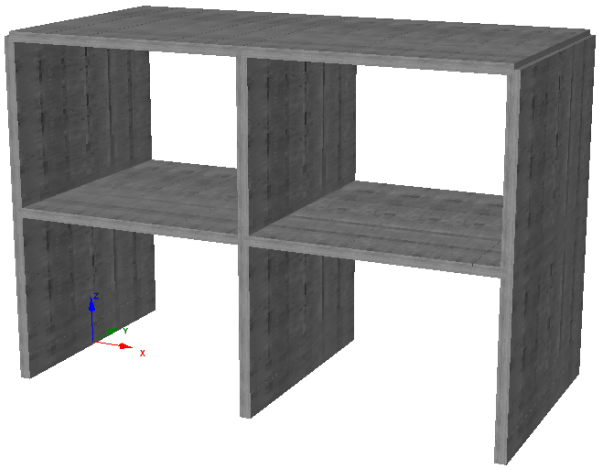

Figure 2.16: SeismoStruct model of the cast-in-place RC wall-slab building

2.4.1 Modelling assumptions

Table 2.9 summarises the main characteristics and modelling assumptions for this type of structural typology.

Table 2.9: CIP RC Wall-Slab Building – Summary of the building model information

Typology (v3 | v5)	REST-URM-A | UBH-CR-CIP/LWAL/CR-CIP/LN/EW/FC
Number of storeys	2 storeys
Height	5.56 m
Directions	Weak = party walls act out of plane, Strong = party walls act in plane
Walls	180 mm thick walls modelled as a series of displacement-based fibre beam elements with material properties that are calibrated according to material characterisation testing (see Eucentre 2017c).
Floors	160 mm thick walls modelled as a series of displacement-based fibre beam elements with material properties that are calibrated according to material characterisation testing (see Eucentre 2017c).
Floor to wall connection	Connections between foundation/slabs and transverse walls are modelled by means of 100 mm long inelastic displacement-based fibre beam elements, with material properties that are calibrated in accordance to both material characterisation testing and observations from the full-scale test (i.e. sliding of smooth starter rebars at the foundation level).
Total mass (weight)	75 t
Footprint area	32 m^2
Concrete material properties	Material mechanical properties were inferred considering the parameters provided in Eucentre (2017c); it is nonetheless noted that material properties of concrete have limited influence on the response of this type of structures, whose seismic response is mostly governed by the rocking at the base of the walls (and associated sliding of the smooth starter bars at the foundation).

As mentioned previously, results from a cyclic test on a full-scale test specimen that was based on the prototype structure being analysed herein were available and employed in the validation/calibration of the modelling strategy and assumptions summarised in Table 2.9 above – a comparison between the experimental and numerical results is shown in Figure 2.17, taken from the report by Brunesi and Nascimbene (2017).

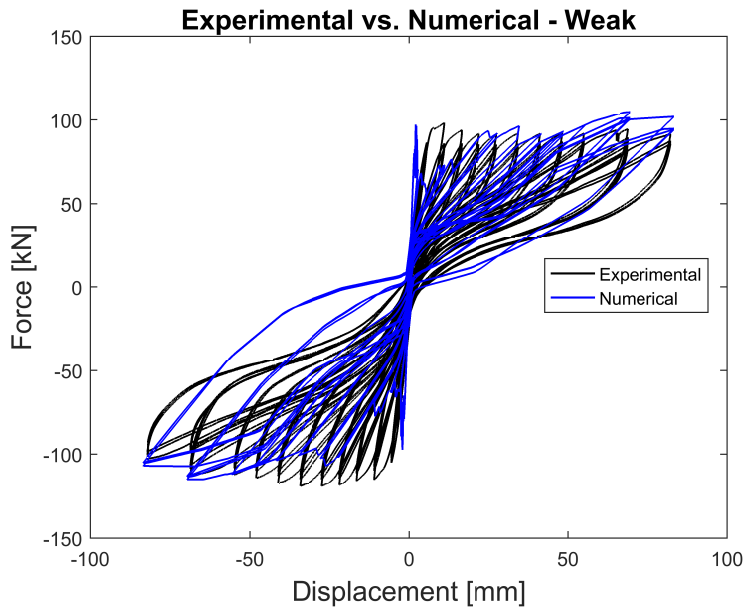

Figure 2.17: CIP RC Wall-Slab Building – Comparison between experimental and numerical results

2.4.2 Summary of results

Displacement and base shear results for the weak and strong directions are summarised in Table 2.10. Collapse was not observed in any of the analyses, but the hysteretic response was nevertheless useful for calibrating the SDOF model used in the fragility function development (Crowley and Pinho, 2017). The hysteresis plots of all 11 records are shown in Figure 2.18 and Figure 2.19 for the weak and strong directions, respectively.

Table 2.10: CIP RC Wall-Slab building – Summary of the numerical results

Ground motion	AvgSa [g]	Weak direction		Strong direction	
		Peak ref. node displacement (pre-collapse*) [mm]	Peak base shear (pre-collapse*) [kN]	Peak ref. node displacement (pre-collapse*) [mm]	Peak base shear (pre-collapse*) [kN]
N_00356L	0.07	8	77	0.0	97
E_00137_EW	0.09	11	84	0.1	229
N_00694T	0.14	21	115	0.2	187
N_00616T	0.22	38	120	0.1	240
N_00147T	0.27	54	125	0.2	209
N_00250L	0.34	57	124	0.5	456
E_17167_EW	0.40	80	163	0.7	370
N_00415L	0.46	129	182	1.8	675
N_00569T	0.46	212	227	3.5	360
N_00407L	0.57	82	185	0.9	366
N_00451T	0.74	199	234	4.1	521

* pre-collapse response values stand for: (i) either peak values observed during the entire analyses when no collapse occurs, or (ii) response values at the instant immediately before collapse occurs

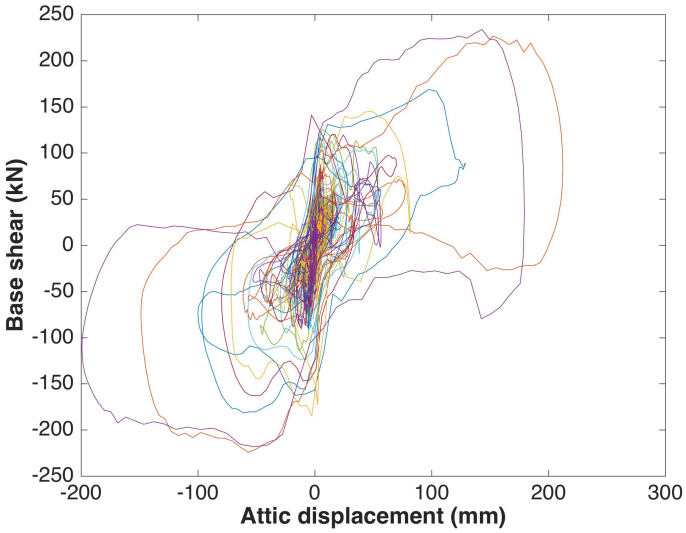

Figure 2.18: CIP RC Wall-Slab Building – Hysteresis plots of the 11 recordings in the weak direction

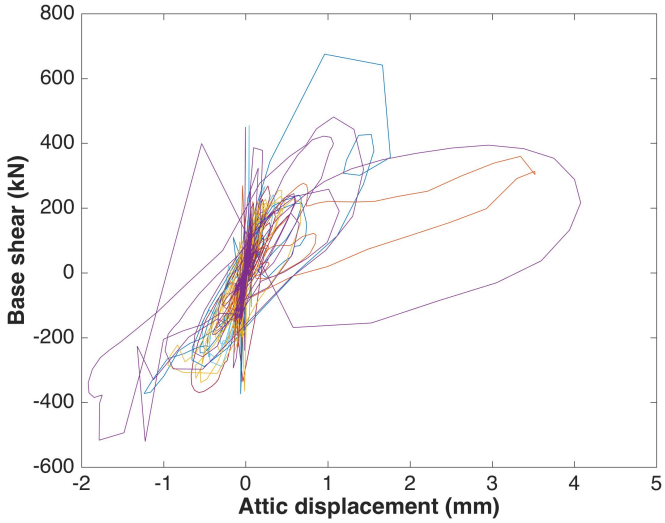

Figure 2.19: CIP RC Wall-Slab Building – Hysteresis plots of the 11 recordings in the strong direction

3 Existing Index Building Models and Results

In order to provide calibration data for the SDOF models of steel and timber buildings, nonlinear dynamic analyses of two index buildings that were previous modelled (and subjected to nonlinear static analysis) by Mosayk have been undertaken. The details of these models are provided in detail in Mosayk (2015), and so only the results are provided herein.

3.1 Timber frame/panel

Timber frame buildings, characterised by an internal load-bearing timber frame and an outer brick façade, have been represented by the building and model shown in Figure 3.1. The external walls were not included in the model, but the stiffness contribution of plasterboard panels was modelled. The structure is very regular and both directions have similar stiffness and strength; the "weak" and "strong" direction terminology is thus only used in the next section for consistency with the other sections.

Figure 3.1: Kwelder 8 timber frame/panel house from Google Street View (left) and the corresponding SeismoStruct model (right)

3.1.1 Summary of results

Displacement and base shear results for the weak and strong directions are summarised in Table 3.1. Collapse was not reached during the dynamic analysis, and so the results of the nonlinear static analysis (described in Mosayk, 2015) have been used to identify the ultimate displacement capacity of the model. The hysteresis plots of all 11 records are shown in Figure 3.2 and Figure 3.3 for the weak and strong directions, respectively; as mentioned previously, these results have been used to calibrate the SDOF model for timber buildings (Crowley and Pinho, 2017).

Table 3.1: Timber frame building – Summary of the numerical results

Ground motion	AvgSa [g]	Weak direction		Strong direction	
		Peak ref. node displacement (pre-collapse*) [mm]	Peak base shear (pre-collapse*) [kN]	Peak ref. node displacement (pre-collapse*) [mm]	Peak base shear (pre-collapse*) [kN]
N_00356L	0.07	2.6	34	2.7	26
E_00137_EW	0.09	7.8	53	7.8	72
N_00694T	0.14	8.9	52	5.4	65
N_00616T	0.22	17.0	64	4.7	57
N_00147T	0.27	10.4	64	5.4	65
N_00250L	0.34	32.4	84	13.5	78
E_17167_EW	0.40	36.2	88	17.3	82
N_00415L	0.46	26.7	82	36.3	85
N_00569T	0.46	57.4	90	13.5	75
N_00407L	0.57	49.0	89	14.3	81
N_00451T	0.74	121.7	90	46.6	84

* pre-collapse response values stand for: (i) either peak values observed during the entire analyses when no collapse occurs, or (ii) response values at the instant immediately before collapse occurs

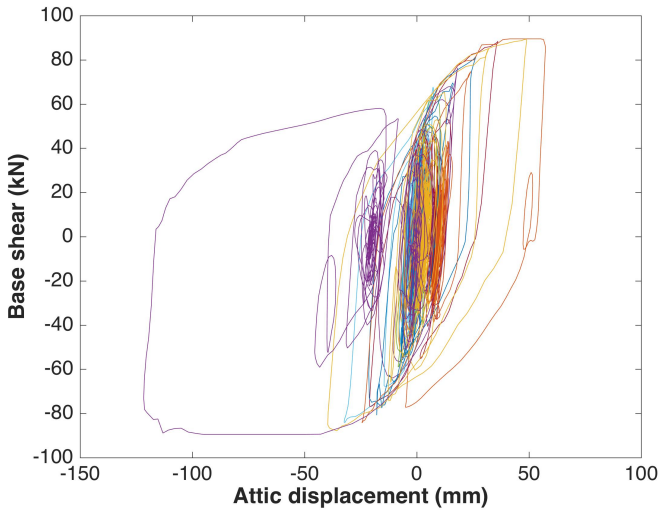

Figure 3.2: Timber frame building – Hysteresis plots of the 11 recordings in the weak direction

3.2 Light steel braced frame

Light steel braced frames are typically used for industrial buildings and the index building that has been used to represent this typology has five steel portal frames along the longitudinal direction and steel braced frames in the transverse direction (see Figure 3.4). The weak direction (identified from the pushover analyses presented in Mosayk, 2015) is the direction with bracing.

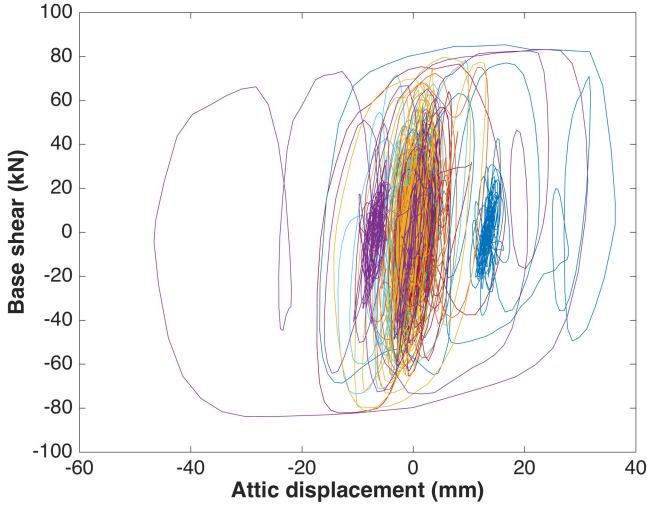

Figure 3.3: Timber frame building – Hysteresis plots of the 11 recordings in the strong direction

Figure 3.4: Beneluxweg 15 light steel braced frame from Google Street View (top) and the corresponding SeismoStruct model (bottom)

3.2.1 Summary of results

Displacement and base shear results for the weak and strong directions are summarised in Table 3.2. Collapse was not reached during the dynamic analysis, and so the results of the nonlinear static analysis (described in Mosayk, 2015) have been used to identify the ultimate displacement capacity of the model. The hysteresis plots of all 11 records are shown in Figure 3.5 and Figure 3.6 for the weak and strong directions, respectively. Although these results do not provide significant nonlinearity, they have been used by Crowley and Pinho (2017) to calibrate the SDOF model for steel buildings, and the backbone curves have been taken from the pushover analyses.

Table 3.2: Steel braced frame – Summary of the numerical results

Ground motion	AvgSa [g]	Weak direction		Strong direction	
		Peak ref. node displacement (pre-collapse*) [mm]	Peak base shear (pre-collapse*) [kN]	Peak ref. node displacement (pre-collapse*) [mm]	Peak base shear (pre-collapse*) [kN]
N_00356L	0.07	0.9	18	25.6	30
E_00137_EW	0.09	1.8	35	32.4	56
N_00694T	0.14	1.9	37	43.9	90
N_00616T	0.22	2.6	53	25.3	27
N_00147T	0.27	2.8	50	28.0	36
N_00250L	0.34	5.1	85	48.8	130
E_17167_EW	0.40	5.0	124	80.5	188
N_00415L	0.46	5.2	97	75.1	184
N_00569T	0.46	7.6	116	46.4	115
N_00407L	0.57	8.0	159	37.8	93
N_00451T	0.74	12.4	199	56.3	158

* pre-collapse response values stand for: (i) either peak values observed during the entire analyses when no collapse occurs, or (ii) response values at the instant immediately before collapse occurs

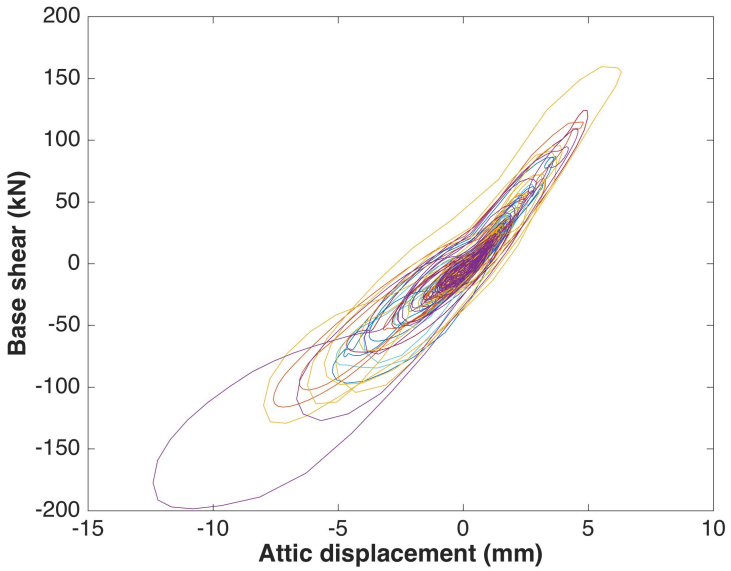

Figure 3.5: Steel braced frame – Hysteresis plots of the 11 recordings in the weak direction

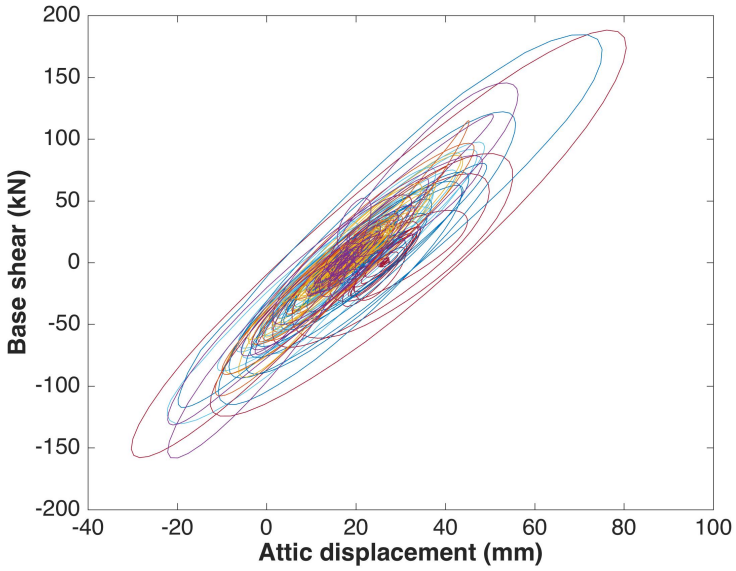

Figure 3.6: Steel braced frame – Hysteresis plots of the 11 recordings in the strong direction

4 Closing Remarks

Using two software packages (ELS and SeismoStruct) whose capacity in prediction the seismic response of structures from the Groningen region has been validated through comparisons and calibration against experimental results, nonlinear dynamic analyses of a number of index buildings or structures were carried out.

The corresponding results, in the form of base-shear vs. attic displacement hysteretic plots, were then provided to NAM's Fragility Modelling Team, so that these could be used in the development of the fragility and consequences models used in NAM's v5 hazard and risk assessment.

References

GENERAL

Arup (2017a) "Typology Modelling: Analysis Results in Support of Fragility Functions – 2017 Batch Results," *Report n. 229746_031.0_REP2005*, Amsterdam, The Netherlands.

Arup (2017b) "EDB V5 post-analysis documentation," *Report n. 229746_052.0_REP2018c*, Amsterdam, The Netherlands.

Arup (2017c) "LNEC-BUILD-1: Modelling Predictions and Analysis Cross Validation," *Report n. 229746_031.0_REP2004*, Amsterdam, The Netherlands.

Arup (2017d) "EUC-BUILD-4 Prototype building description," *Report n. 229746_031_NOT2008_Rev0.05_Issue*, Amsterdam, The Netherlands.

Arup (2017e) "EUC-BUILD-3 Prototype building description," *Report n. 229746_031_NOT2007_Rev0.06_Issue*, Amsterdam, The Netherlands.

Brunesi E., Nascimbene R. (2017) "Numerical modelling and analysis of a full-scale reinforced concrete wall-slab-wall structure representative of the Groningen building stock," *Report n. EUC096/2017U*, European Centre for Training and Research in Earthquake Engineering (EUCENTRE), Pavia, Italy.

Brunesi E., Peloso S., Pinho R., Nascimbene R. (2017a) "Cyclic testing of a full-scale two-storey RC precast wall-slab-wall structure representative of the Groningen building stock," *Report n. EUC173/2017U*, European Centre for Training and Research in Earthquake Engineering (EUCENTRE), Pavia, Italy. Available from URL: http://www.eucentre.it/nam-project

Brunesi E., Peloso S., Pinho R., Nascimbene R. (2017b) "Dynamic testing of a full-scale two-storey RC precast wall-slab-wall structure representative of the Groningen building stock," European Centre for Training and Research in Earthquake Engineering (EUCENTRE), Pavia, Italy. Available from URL: http://www.eucentre.it/nam-project

Brunesi E., Peloso S., Pinho R., Nascimbene R. (2017c) "Cyclic testing of a full-scale cast-in-place RC wall-slab-wall structure representative of the Groningen building stock," *Report n. EUC095/2017U*, European Centre for Training and Research in Earthquake Engineering EUCENTRE, Pavia, Italy. Available from URL: http://www.eucentre.it/nam-project

Crowley H. and Pinho R. [2017] "Report on the v5 fragility and consequence models for the Groningen Field.," Pavia, Italy.

Kohranghi M., Bazzurro P., Vamvatsikos D., Spillatura A. (2017) "Conditional spectrum-based ground motion record selection using average spectral acceleration," *Earthquake Engineering and Structural Dynamics*, Vol. 46, No. 10, pp. 1667-1685.

Meguro K., Tagel-Din H. (2000) "Applied Element Method for structural analysis: Theory and application for linear materials," *JSCE International Journal of Structural Engineering and Earthquake Engineering*, Vol. 17, No. 1, pp. 21–35.

Meguro K., Tagel-Din H. (2001) "Applied Element simulation of RC Structures under cyclic loading," *ASCE Journal of Structural Engineering*, Vol. 127, No. 11, pp. 1295-1305.

Meguro K., Tagel-Din H. (2002) "Applied Element Method used for large displacement structure analysis," *Journal of Natural Disaster Science*, Vol. 24, No. 2, pp. 65-82.

Mosayk (2014) "Software verification against experimental benchmark data," Pavia, Italy.

Mosayk (2015) "Structural modelling of non-URM buildings – v2 risk model update," Pavia, Italy.

Mosayk (2016) "Using the Applied Element Method to model URM walls subjected to in-plane cyclic shear-compression," Pavia, Italy.

Mosayk (2017a) "Using the Applied Element Method to model the shake-table testing of two full-scale URM houses," Pavia, Italy.

Mosayk (2017b) "Using the Applied Element Method to model the collapse shake-table testing of a URM cavity wall structure," Pavia, Italy.

Mosayk (2017c) "Using the Applied Element Method to model the collapse shake-table testing of a terraced house roof substructure," Pavia, Italy.

Mosayk (2017d) "Using the Applied Element Method to model URM walls subjected to out-of-plane shake-table testing," Pavia, Italy.

Tomassetti U., Correia A.A., Graziotti F., Marques A.I., Mandirola M. and Candeias P.X. (2017) "Collapse shaking table test on a URM cavity wall building representative of a Dutch terraced house," European Centre for Training and Research in Earthquake Engineering (EUCENTRE), Pavia, Italy.

SOFTWARE TOOLS

ASI (2017) *Extreme Loading for Structures v5*, Applied Science International LLC., Durham (NC), USA.

Seismosoft (2017) *SeismoStruct v2016 – A computer program for static and dynamic nonlinear analysis of framed structures*, available from http://www.seismosoft.com